Research paper

The Holocene
2018, Vol. 28(7) 1082–1092

DOI: 10.1177/0959683618761542
journals.sagepub.com/home/hol
SAGE

The manifestation of the Younger Dryas event in the East Asian summer monsoon margin: New evidence from carbonate geochemistry of the Dali Lake sediments in northern China

Jiawei Fan,[1,2] Jule Xiao,[1,2,3] Ruilin Wen,[1,2] Shengrui Zhang,[1,2] Xu Wang,[1,2] Linlin Cui,[1,2] Yanhong Liu,[4] He Li[4] and Jiaojiao Yue[5]

Abstract

The processes and mechanisms of the Younger Dryas (YD) event in the modern northern margin of the East Asian summer monsoon (EASM) are still heatedly debated. This study presents new high-resolution (~25 years) records of elements and stable isotopes of <38-μm calcites from a sediment core from Dali Lake in order to investigate the climatic change in the EASM margin at the last glacial–interglacial transition. The <38-μm calcites in the Dali Lake sediments are cubical or rhombohedral, implying that they are predominated by endogenic calcites precipitated within the water body of the lake. High values of Ca and Mg concentrations of the endogenic calcites are interpreted as strong evaporation and low dissolved CO_2 concentration of the lake water related to high regional temperature. Concurrent increases in $\delta^{13}C$ and $\delta^{18}O$ values of the endogenic calcites are interpreted as the result of intensified evaporation associated with high temperature or low precipitation in the region. These data indicate that the climate in the Dali Lake region was relatively warm and wet from 15,500 to 12,800 and from 11,550 to 10,000 cal. yr BP, and cold and dry from 12,800 to 11,550 cal. yr BP, which was generally supported by the evidence from the data of sedimentary organic matter from the same sediment core. In addition, the abruptness of the temperature change in the Dali Lake region from 12,800 to 11,550 cal. yr BP could be corresponded, within age uncertainties, to the YD cold reversal occurring over northern high latitudes. The atmospheric coupling between the North Atlantic region and the EASM margin was proposed as the dominant pattern influencing the climatic change in the Dali Lake region during the YD event.

Keywords

East Asian summer monsoon, endogenic calcite, Northern China, paleoprecipitation, paleotemperature, Younger Dryas

Received 20 June 2017; revised manuscript accepted 30 January 2018

Introduction

The Younger Dryas (YD) event, a severe cold reversal that interrupted the global warming during the last deglaciation, had drawn great attention from the paleoclimatologists (e.g. Bond et al., 1997; Dansgaard et al., 1993; Heinrich, 1988). It was suggested that significant weakening of the North Atlantic meridional overturning circulation (AMOC) which might have been triggered by a large amount of Arctic meltwater input (Broecker et al., 1989; McManus et al., 2004; Tarasov and Peltier, 2005) caused significant temperature decreases of 10–15°C in the Greenland region during the YD period (Alley, 2000; Johnsen et al., 2001; Severinghaus et al., 1998). Previous studies emphasized the influence of bipolar seesaw driven by the reduction in AMOC on the opposite trends of temperature changes between Northern and Southern Hemispheres (NH and SH) during the YD period (e.g. Shakun and Carlson, 2010). However, it is still unclear whether such a change in the oceanic circulation or a modification of atmospheric circulation patterns related to northern high latitude cooling could play a key role in the climatic changes in the continental interior (Duan et al., 2016; Mikolajewicz et al., 1997; Wunsch, 2006).

[1]Key Laboratory of Cenozoic Geology and Environment, Institute of Geology and Geophysics, Chinese Academy of Sciences, China
[2]Institutions of Earth Science, Chinese Academy of Sciences, China
[3]College of Earth Sciences, University of Chinese Academy of Sciences, China
[4]State Key Laboratory of Lithospheric Evolution, Institute of Geology and Geophysics, Chinese Academy of Sciences, China
[5]School of Earth Sciences, China University of Geosciences, China

Corresponding authors:
Jiawei Fan, Key Laboratory of Cenozoic Geology and Environment, Institute of Geology and Geophysics, Chinese Academy of Sciences, Beijing 100029, China.
Email: jwfan@mail.iggcas.ac.cn

Jule Xiao, Key Laboratory of Cenozoic Geology and Environment, Institute of Geology and Geophysics, Chinese Academy of Sciences, Beijing 100029, China.
Email: jlxiao@mail.iggcas.ac.cn

In the Asian monsoonal region, there have been numerous studies of moisture changes during the YD period (e.g. An et al., 2012; Chen et al., 2015; Hong et al., 2010; Huang et al., 2012; Liu et al., 2008; Qiang et al., 2013; Russell et al., 2014; Shen et al., 2005; Stebich et al., 2011; Yancheva et al., 2007; Yang et al., 2016; Zhou et al., 2016); however, these results exhibit significant spatial differences. For example, the $CaCO_3$ record from Qinghai Lake on the northeastern Tibetan Plateau (An et al., 2012) suggested a dry climate during the YD period, which was interpreted as a response of the modification of atmospheric circulation patterns related to significant cooling in northern high latitudes (An et al., 2012), while the lipid-based paleohydrological record from Dajiuhu peatland in the middle reaches of the Yangtze River (Huang et al., 2012) indicated an increased precipitation during that time, in response to the southward migration of the western Pacific subtropical high related to the decreases in the sea surface temperature (SST) in the western Pacific warm pool (WPWP) (Huang et al., 2012). In view of the uncertainties of a single proxy indicator and the inherent complexities in the interactions between different climatic factors such as precipitation, temperature, and evaporation, multidisciplinary investigations of records from the Asian monsoonal region are needed to provide more insights into the changes in each climatic factor and its possible driving mechanism during the YD period.

Dali Lake is located in the modern northern margin of the East Asian summer monsoon (EASM), where the regional climate is highly sensitive to the East Asian monsoon (EAM) (An, 2000). Endogenic carbonates precipitated in Dali Lake can provide important information on past changes in regional climate (Fan et al., 2016). This study presents high-resolution (~25 years) records of elements and stable isotopes of <38-μm calcites (endogenic calcites) from a sediment core from Dali Lake during the interval from 15.5 to 10 cal. kyr BP. These new data, together with previously published data of TOC and TN concentrations (Fan et al., 2017) from the same sediment core, would enhance our knowledge of the climate history in the EASM margin during the last deglaciation and improve our understanding of the potential driving mechanisms of the EASM variability during the YD period.

Study area

Geography

Dali Lake (43°13′–43°23′ N, 116°29′–116°45′ E) is located in the northern margin of the E–W-extending Hulandaga Desert Land, 70 km west of Hexigten Banner, Inner Mongolia (Figure 1), in an inland fault-depression basin that was formed in the Pliocene to Pleistocene (Li, 1993). The lake has an area of 238 km^2, a maximum water depth of 11 m, an elevation of 1226 m above sea level (Figure 1), and is hydrologically closed. Hills of basaltic rocks surround the lake to the north and west, lacustrine plains are present along the eastern shore, and there is no outcrop of carbonate rocks in the catchment. Two permanent rivers, the Gongger and Salin Rivers, enter the lake from the northeast, and two intermittent streams, the Holai and Liangzi Rivers, enter from the southwest (Figure 1); however, there are no outflowing rivers. The Gongger River, the major inflow, rises in the southern terminal part of the Great Hinggan Mountains, where the elevation reaches 2029 m, and has a drainage area of 783 km^2 and a total channel length of 120 km (Li, 1993).

Climate

Dali Lake sits at the transition from semi-humid to semi-arid areas of the middle temperate zone. The climate of the region is mainly controlled by the EAM. In region, mean annual temperature is 3.2°C with a July average of 20.4°C and a January average of −16.6°C (Figure 2). Mean annual precipitation (MAP) is 383 mm, and ~70% of the annual precipitation falls from June to August (Figure 2). Mean annual evaporation reaches 1632 mm, which is more than four times the annual precipitation (Figure 2).

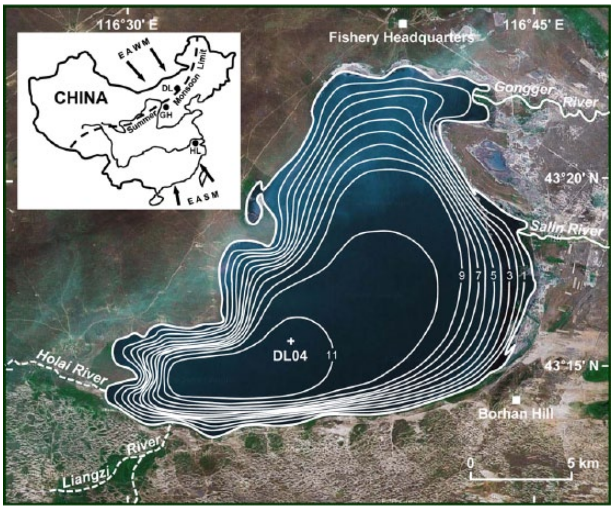

Figure 1. Map of Dali Lake (from http://maps.google.com) showing the location of the DL04 sediment core (cross). The bathymetric survey of the lake was conducted in June 2002 using a FE-606 Furuno Echo Sounder (contours in m). The inset map shows the core locations of Dali Lake (DL) (43°15′ N, 116°36′ E), Gonghai Lake (GH) (38°54′ N, 112°14′ E), and Hulu Cave (HL) (32°30′ N, 119°10′ E) in China (solid circles) and the modern northern limit of the East Asian summer monsoon defined by the 400-mm isohyet of mean annual precipitation (Xiao et al., 2004).

Water chemistry

The water of Dali Lake at present has an average pH of 9.5, an average salinity of 7.4 g/L, and an average alkalinity of 4.9 $CaCO_3$ g/L (Fan et al., 2016) (Table 1). The lake water contains major cations (average values) of Ca^{2+} (5.5 mg/L), Mg^{2+} (33.7 mg/L), K^+ (266.3 mg/L), and Na^+ (2516.7 mg/L), and major anions (average values) of CO_3^{2-} (644.3 mg/L), HCO_3^- (2336.0 mg/L), SO_4^{2-} (403.0 mg/L), and Cl^- (1753.3 mg/L) (Fan et al., 2016). The Mg/Ca mole ratio of lake water averages 8.3 (Fan et al., 2016). The $\delta^{18}O$ and δ^2H values of lake water average −2.1‰ and −22.5‰, respectively, while the $\delta^{13}C_{DIC}$ averages −0.3‰ (Fan et al., 2016) (Table 1). Data of chemical properties of water sampled from the inflowing rivers to the lake are shown in Table 1.

Materials and methods

Sediment coring and lithology

The DL04 core (43°15.68′ N, 116°36.26′ E) was extracted to a total depth of 11.83 m beneath the lake floor in the depocenter of Dali Lake (Xiao et al., 2008). The 7.71–11.83 m of the DL04 core is used for the present study (Figure 3). The sediments consist of blackish-gray to greenish-gray, massive silt, and can be divided into four main sedimentary units (Figure 3), as follows: 1183–985 cm blackish-gray massive silt with greenish-gray bands at depths of 1183–1113 cm, 985–875 cm grayish-black massive silt, 875–789 cm blackish-gray massive silt, and 789–770 cm greenish-gray massive silt with occasional blackish-gray bands.

Chronology

In this study, the reservoir-corrected radiocarbon dates and age–depth model of the 7.71–11.83 m of the DL04 core are cited from Fan et al. (2017) (Figure 3; Table 2). The reservoir effect of Dali

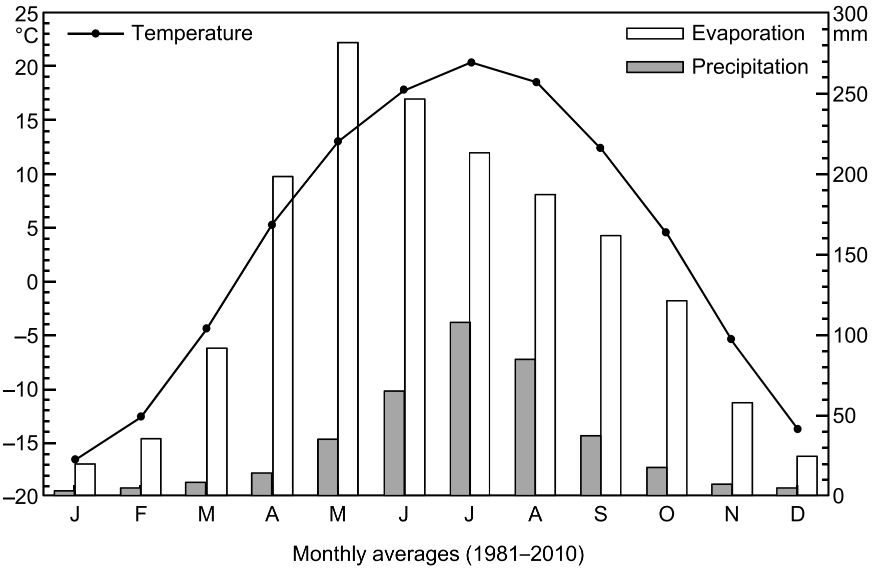

Figure 2. Mean monthly temperature, mean monthly precipitation, and mean monthly evaporation in the Dali Lake region. Data are the averages of observations from 1981 to 2010 at Hexigten Banner Meteorological Station, 70 km east of Dali Lake (unpublished data courtesy of Inner Mongolia Meteorological Bureau).

Table 1. Chemical characteristic of water samples from Dali Lake and from the inflowing rivers.

Water sample	pH	T (°C)	Salinity (g/L)	Alkalinity ($CaCO_3$ g/L)	Ca^{2+} (mg/L)	Mg^{2+} (mg/L)	K^+ (mg/L)	Na^+ (mg/L)	CO_3^{2-} (mg/L)	HCO_3^- (mg/L)	SO_4^{2-} (mg/L)	Cl^- (mg/L)	$\delta^{18}O$ (‰)	δD (‰)	$\delta^{13}C_{DIC}$ (‰)
Dali Lake[a]	9.3	16.0	9.2	5.0	7.2	50.2	410.0	3120.0	643.0	2415.0	388.0	1710.0	−2.1	−20.3	−0.2
Dali Lake[b]	9.6	17.3	7.5	4.7	4.7	21.6	152.0	2360.0	622.0	2253.0	396.0	1740.0	−2.2	−24.3	−0.7
Dali Lake[c]	9.6	14.1	5.5	4.9	4.7	29.4	237.0	2070.0	668.0	2340.0	425.0	1810.0	−2.1	−22.8	−0.1
Gongger River[d]	8.3	0.6	0.2	0.2	18.8	6.3	2.6	18.4	0	135.2	15.4	8.5	−15.3	−108.0	−6.3
Gongger River[e]	8.7	21.6	0.2	0.2	30.0	8.4	2.6	16.6	6.1	126.6	7.1	6.5	−10.8	−80.9	−9.3
Salin River[d]	9.0	10.5	0.5	0.5	21.2	25.5	8.1	62.1	12.4	290.9	10.2	24.5	−4.6	−42.1	2.5
Salin River[e]	7.9	21.0	0.4	0.4	21.2	23.1	10.8	55.8	0	256.2	9.2	20.4	−3.4	−36.6	−2.0
Liangzi River[d]	8.1	0.5	0.2	0.2	15.1	7.2	1.8	15.4	0	138.4	5.1	4.6	−10.1	−71.7	−6.2
Liangzi River[e]	7.4	15.7	0.2	0.2	30.6	9.4	4.1	15.8	0	151.2	5.9	5.1	−10.2	−71.8	−9.7
Holai River[d]	8.5	1.9	0.3	0.3	17.2	13.3	2.1	25.0	0	188.7	11.6	8.0	−9.2	−74.7	−7.6
Holai River[e]	7.9	14.1	0.3	0.4	36.5	17.5	5.1	23.9	0	219.2	12.8	8.8	−10.2	−69.8	−10.5

[a,b,c]Sampled in June 2010 from the central-northwestern, central-northeastern and central-southern parts of the lake.
[d]Sampled during spring floods in April 2011.
[e]Sampled during summer floods in August 2011.
The original data are cited from Fan et al. (2016).

Lake may have changed in different periods but it is difficult to obtain absolutely accurate dates because there is little terrestrial macrofossil or plant debris in the core sediments for accurate dating. The age–depth model indicates that the 7.71–11.83 m of the DL04 core covered the last deglaciation from 16 to 10 cal. kyr BP (Fan et al., 2017) (Figure 3; Table 2). The sedimentation rates of ca. 50–120 cm/kyr and sampling intervals of 1–3 cm in the present study provide potential temporal resolutions of ~25 years for the geochemical data.

X-ray diffractometry and scanning electron microscope analyses

Six representative bulk sediment samples are selected from the depths of 8.14 m (10.97 kyr BP), 8.17 m (11.01 kyr BP), 8.93 m (11.91 kyr BP), 8.95 m (11.93 kyr BP), 10.68 m (13.87 kyr BP), and 10.96 m (14.41 kyr BP) of the DL04 core and used for x-ray diffractometry (XRD) analyses. The compositions of minerals are determined with a Rigaku D/MAX–2400 XRD equipped with a graphite monochromator. Each sample is spread and leveled onto a 2 × 1.5 cm^2 concave glass plate for determinations with the XRD. The XRD employs the radiation of a Cu target at 40 KV, 60 mA to generate x-ray that irradiates a sample at a scanning angle of 2θ (2θ = 3°–70°) and produces the diffraction peaks of the sample. These peaks are filtered and monochromatized through the graphite monochromator, resulting in the characteristic diffraction peaks of minerals comprising the sample. The compositions of minerals in a sample are determined by comparison of the sample's characteristic diffraction peaks with the standard card spectrum. Major peaks around 3.03 Å (29.42° 2θ) reflect the dominance of calcite. These six bulk sediment samples are sieved through a 400-mesh (38-μm pore size) sieve to obtain the <38-μm fractions, and the <38-μm sediments are used for the scanning electron microscope (SEM) analyses with a LEO1450VP SEM.

Elemental and isotopic analyses

The carbonate-rich horizons of the 7.71–11.83 m of the DL04 core are sampled at 1- to 3-cm intervals for the analyses of Ca and

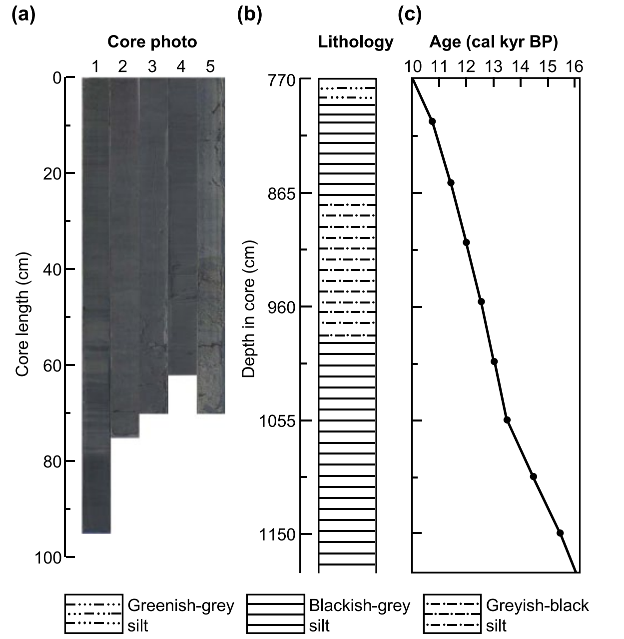

Figure 3. (a) Photograph of the 7.11–11.83 m of the DL04 core. The first section is the interval 711–806 cm, and the fifth section is the interval 1113–1183 cm. (b) Lithology of the 7.71–11.83 m of the DL04 core. (c) Age–depth model for the 7.71–11.83 m of the DL04 core. Solid circles represent the mean values of 2σ ranges of calibrated ages of reservoir-corrected radiocarbon dates (Fan et al., 2017).

Mg concentrations and δ18O and δ13C values of the <38-μm carbonates (n = 212). The bulk sediment samples are sieved through a 400-mesh to obtain the <38-μm fractions.

The Ca and Mg concentrations of the carbonates in <38-μm sediments are determined with an ICP-OES. Each sample of 100 mg of <38-μm sediments is pre-treated with 40 mL of 1% acetic acid, and the acetic acid solution is diluted 1000 times with nitric acid solution for measurements of Ca and Mg concentrations (Fan et al., 2016). The relative error was less than 5% for both Ca and Mg concentrations. Ca and Mg concentrations are expressed in weight percentages in <38-μm sediments of a sample.

The δ18O and δ13C values of the carbonates in <38-μm sediments are determined with a Finnigan MAT 253 mass spectrometer equipped with a Gas Bench-II carbonate preparation device. Each sample of ~2 mg of <38-μm sediments is added by 50 μL of 103% H_3PO_4, and the sample solution is kept for reaction in Gas Bench-II at 72°C for 1 h to generate an appropriate amount of CO_2 for measurements of $^{18}O/^{16}O$ and $^{13}C/^{12}C$ ratios (Fan et al., 2016). The precision is better than 0.1‰ for δ18O and 0.2‰ for δ13C values.

Numerical analyses

Cluster analysis (CONISS, Grimm, 1987) is used to statistically divide the zonation of the time series of Ca and Mg concentrations and δ18O and δ13C values of <38-μm carbonates for the DL04 core from 15,500 to 10,000 cal. yr BP. All the raw data of geochemical proxies are normalized, and then CONISS is conducted on the normalized data. CONISS is based on the total sum of squares (Grimm, 1987).

Results

The XRD and SEM results exhibit the dominance of calcites (including calcite and Mg-calcite) in the Dali Lake sediments (Figures 4 and 5). The calcites or calcite aggregates in the <38-μm sediments are cubical or rhombohedral, and the calcite crystals are granular and lenticular (Figure 5). The calcite content is close to zero from 16,000 to 15,500 cal. yr BP. The Ca and Mg concentrations and δ18O and δ13C values of <38-μm calcites from 15,500 to 10,000 cal. yr BP are plotted in Figure 6. Ca and Mg concentrations vary from 0.20% to 4.93% and from 0% to 1.25%, respectively. δ18O values vary from −7.2‰ to −2.3‰, and δ13C values vary from −2.3‰ to 3.4‰. The time series of Ca and Mg concentrations and δ18O and δ13C values from 15,500 to 10,000 cal. yr BP can be divided into four major stages, for example, 15,500–12,800, 12,800–11,550, 11,550–10,900, and 10,900–10,000 cal. yr BP, based on the stratigraphically constrained cluster analysis (CONISS, Grimm, 1987) (Figure 6).

Stage 4 (1150–974 cm, 15,500–12,800 cal. yr BP)

During this stage, Ca and Mg concentrations and δ18O and δ13C values exhibit increasing trends with large fluctuations. They increase from 0.55% to 2.55%, 0.13% to 0.66%, −5.4‰ to −3.7‰, and from −1.5‰ to 1.5‰, respectively, with their most significant peaks of 3.56%, 0.86%, −2.9‰, and 1.6‰ at 14,770 cal. yr BP and most significant troughs of 0.98% and 0.26% for Ca and Mg concentrations at 14,030 cal. yr BP and −4.4‰ and 0.3‰ for δ18O and δ13C values at 14,160 cal. yr BP.

Stage 3 (974–858 cm, 12,800–11,550 cal. yr BP)

This stage is characterized by rapid decreases of Ca and Mg concentrations and δ18O and δ13C values in the beginning. Ca and Mg concentrations decrease rapidly to 15.3%, 0.78%, and 0.24%, respectively, at 12,600 cal. yr BP, and then fluctuate around their averages of 1.50% and 0.38%, respectively, from 12,600 to 11,550 cal. yr BP. δ18O and δ13C values decrease rapidly to −5.5‰ and −0.5‰ at 12,750 cal. yr BP, and then increase rapidly to −3.6‰ and 1.6‰ at 12,725 cal. yr BP; subsequently, δ18O values maintain an average of −3.5‰, while δ13C values exhibit an increasing trend and increase from 1.7‰ to 3.2‰ from 12,725 to 11,550 cal. yr BP.

Stage 2 (858–809 cm, 11,550–10,900 cal. yr BP)

During this stage, Ca and Mg concentrations increase rapidly from 1.18% to 3.54% and 0.33% to 0.78%, respectively. δ18O values maintain an average of −3.2‰. δ13C values exhibit a decreasing trend and decrease from 3.3‰ to 1.2‰.

Stage 1 (809–771 cm, 10,900–10,000 cal. yr BP)

This stage is characterized by rapid and significant decreases of Ca and Mg concentrations and δ18O and δ13C values in the beginning. They decrease to 0.52%, 0.17%, −7.2‰, and −2.3‰, respectively, at 10,760 cal. yr BP, and then increase to 2.30%, 0.52%, −5.5‰, and 2.9‰, respectively, at 10,000 cal. yr BP with their peaks of 3.28%, 0.78%, −4.6‰, and 2.3‰, respectively, at 10,440 cal. yr BP.

Discussion

Implications of the geochemical proxies

Previous studies indicated that the <38-μm carbonates in the upper 6.39 m of the DL04 core were mainly of endogenous origin (Fan et al., 2016), based on the following evidence: (1) The Dali Lake basin is surrounded by hills of basaltic rocks to the west and north, and by mobile sand dunes to the south (Li, 1993), which implies that detrital calcites from the lake catchment should be negligible in the <38-μm carbonates of the lake sediments. (2) SEM images of the <38-μm sediments from two representative samples from the upper 6.39 m of the DL04 core exhibit granular, blocky, lenticular,

Table 2. AMS radiocarbon dates of samples from the 7.71–11.83 m of the DL04 core.

Laboratory number[a]	Depth interval (cm)	Dating material	$\delta^{13}C$ (‰)	^{14}C age (^{14}C yr BP)	Corrected ^{14}C age (^{14}C yr BP)	Calibrated ^{14}C age (2σ) (cal. yr BP)
PLD–12470	799–798	Organic matter	−31.56	9969 ± 32	9497 ± 39	10,869–10,654
PLD–12472	849–848	Organic matter	−30.84	10,464 ± 37	9992 ± 44	11,640–11,267
PLD–12474	899–898	Organic matter	−27.92	10,715 ± 34	10,243 ± 41	12,141–11,805
PLD–12477	950–949	Organic matter	−31.40	11,050 ± 35	10,578 ± 42	12,670–12,515
PLD–12478	999–998	Organic matter	−31.97	11,630 ± 38	11,158 ± 44	13,117–12,898
PLD–12480	1049–1048	Organic matter	−30.63	12,158 ± 37	11,686 ± 44	13,585–13,431
PLD–12483	1100–1099	Organic matter	−27.39	12,876 ± 42	12,404 ± 48	14,818–14,164
PLD–13857	1150–1149	Organic matter	−27.78	13,436 ± 39	12,964 ± 45	15,713–15,290

The original data are cited from Fan et al. (2017).
[a]PLD: Paleo Labo Dating, laboratory code of Paleo Labo Co., Ltd, Japan.

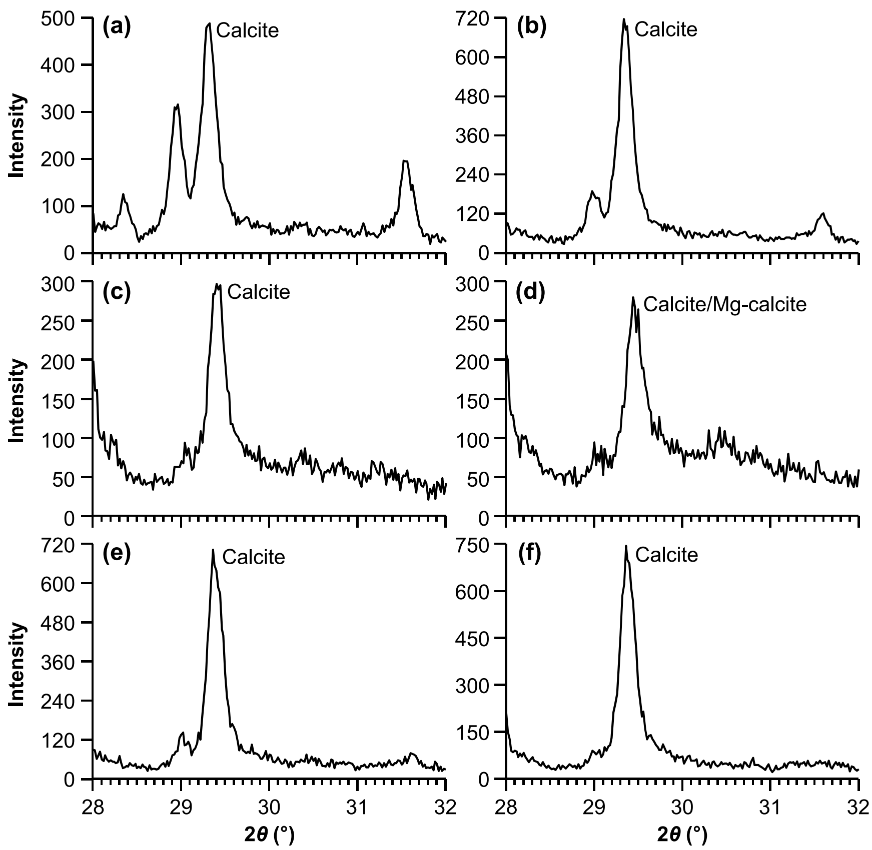

Figure 4. X-ray diffractogram (XRD) (28°–32° 2θ) for six representative bulk sediment samples at the depths of (a) 8.14 m (10.97 kyr BP), (b) 8.17 m (11.01 kyr BP), (c) 8.93 m (11.91 kyr BP), (d) 8.95 m (11.93 kyr BP), (e) 10.68 m (13.87 kyr BP), and (f) 10.96 m (14.41 kyr BP) from the 7.11–11.83 m of the DL04 core. Major peaks occur around 3.03 Å (29.42° 2θ), reflecting dominance of calcite.

and prismatic idiomorphic carbonate crystals, indicating that the carbonate crystals are of endogenous origin and rapidly precipitated. (3) The data of $\delta^{18}O$ values of summer lake water (δw) and of <38-μm calcites (δc) in surface sediments of the lake, and the summer lake water temperature (T) match the paleotemperature equation, for example, $T = 13.8 - 4.58\ (\delta c - \delta w) + 0.08\ (\delta c - \delta w)^2$, for the equilibrium fractionation of calcite precipitation in lake water (Leng and Marshall, 2004). In this study, the calcites from the 7.71–11.83 m of the DL04 core exhibit sharp peaks around 3.03 Å (29.42° 2θ) in the XRD diagram (Figure 4), implying that these calcites are generally well-ordered and less substituted. In addition, the <38-μm calcites or calcite aggregates are cubical or rhombohedral in the SEM images (Figure 5), supporting that they are mainly endogenous in origin (Jiménez-López et al., 2004).

The precipitation of endogenic carbonates in the lake water depends on the balance between ionic activity product (IAP) of Ca^{2+} and CO_3^{2-} and the equilibrium constant K_c (Lerman, 1978). The Ca^{2+} in the lake water is mainly controlled by the Ca^{2+} input for Ca^{2+}-limited saline lakes such as Qinghai Lake (An et al., 2012; Jin et al., 2010), whereas by strong evaporation in brackish lakes such as Daihai Lake (Shen et al., 2002; Xiao et al., 2006). Dali Lake is a brackish lake, and the concentrations of major ions (except for Ca^{2+}) in the lake water are much higher than those in the inflowing rivers (Table 1), suggesting that the strong evaporation of the lake water led to the super-saturation of $CaCO_3$ and the precipitation of Ca^{2+} as calcite (Fan et al., 2016). The CO_3^{2-} in the lake water is mainly controlled by the dissolved CO_2 concentration which is closely related to the lake water temperature and the biological activities (Chen et al., 2016; Liu et al., 2014). The K_c is mainly controlled by the temperature (Lerman, 1978). Previous studies indicated that the precipitation of endogenic calcites in the Dali Lake water was mainly controlled by strong evaporation

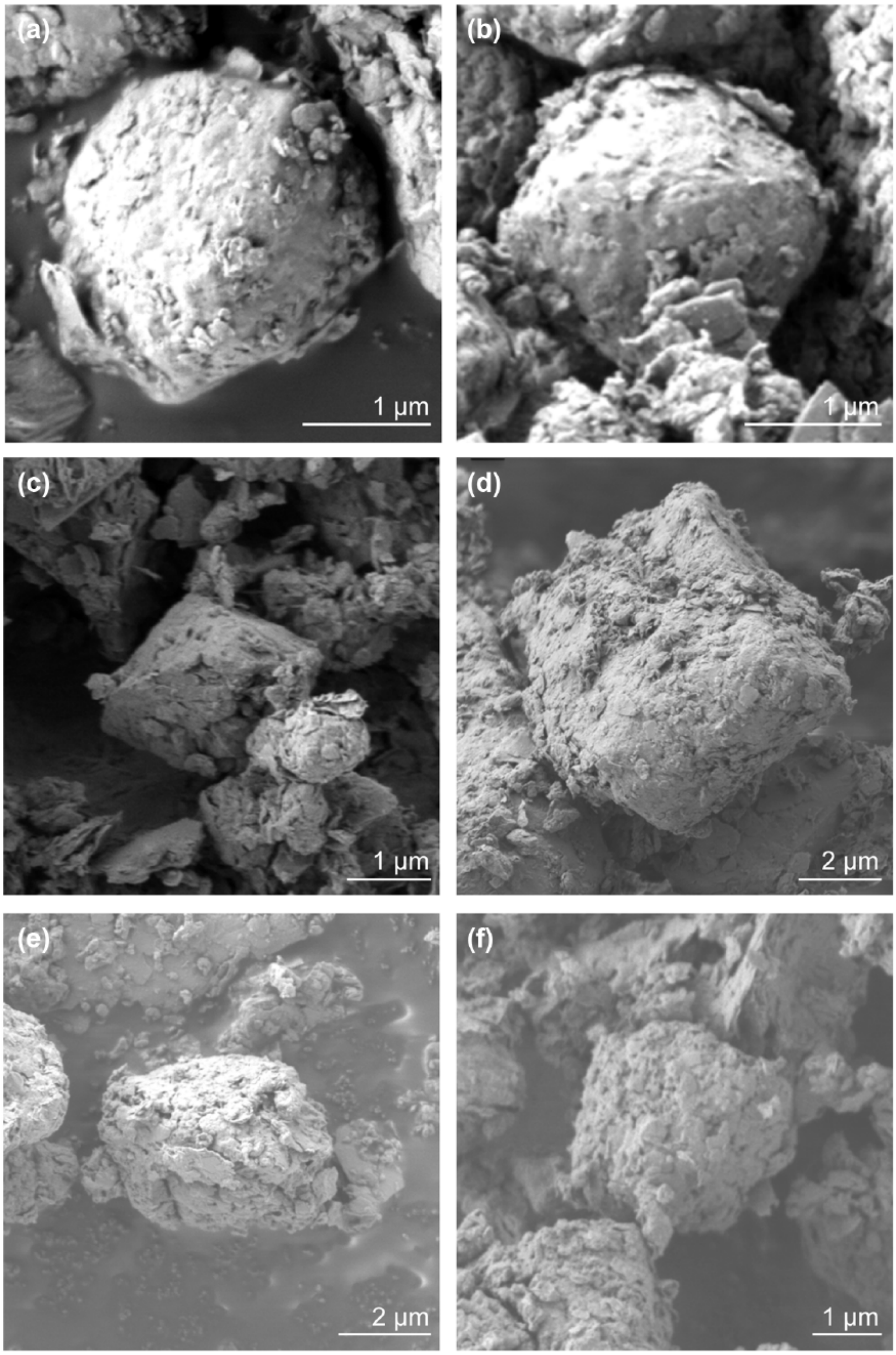

Figure 5. Scanning electron microscope (SEM) images of calcites in the <38-μm sediments from six representative samples at the depths of (a) 8.14 m (10.97 kyr BP), (b) 8.17 m (11.01 kyr BP), (c) 8.93 m (11.91 kyr BP), (d) 8.95 m (11.93 kyr BP), (e) 10.68 m (13.87 kyr BP), and (f) 10.96 m (14.41 kyr BP) from the 7.11–11.83 m of the DL04 core.

related to low precipitation in the region during the last 6000 cal. yr (Fan et al., 2016). The results were supported by multi-proxy data from the same sediment core (Fan et al., 2016). Dali Lake is located in the semi-arid areas, and Ca^{2+} and CO_3^{2-} in the lake water are preferentially precipitated as calcite when evaporation intensifies and dissolved CO_2 concentration decreases, both of which should be mainly controlled by increases in regional temperature during the last deglaciation when biological productivity was generally low and varied in small amplitudes (Fan et al., 2017). In the water of Dali Lake, Mg^{2+} concentrations are much higher than Ca^{2+} concentrations (Table 1), indicating that Mg^{2+} is gradually enriched when Ca^{2+} is precipitated as calcite. Consequently, Mg^{2+} is progressively incorporated into calcite when Mg^{2+}/Ca^{2+} ratio gradually increases (Fan et al., 2016). Therefore, increases in the Ca and Mg concentrations of the endogenic calcites in Dali Lake could indicate increases in regional temperature during the last deglaciation, and vice versa; while significant decreases in the Ca and Mg concentrations during the early Holocene may indicate the fresh water input to the lake overwhelming the evaporative losses (Fan et al., 2016).

The $\delta^{18}O$ values of lacustrine endogenic calcites are a function of the $\delta^{18}O$ values and temperature of the lake water. An increase of 1‰ in the calcite $\delta^{18}O$ values could be caused either by an increase of 1‰ in the water $\delta^{18}O$ values or by a decrease of 4°C (−2.5‰/°C) in the water temperature, or by a combination of both, in the equilibrium of oxygen isotopic fractionation

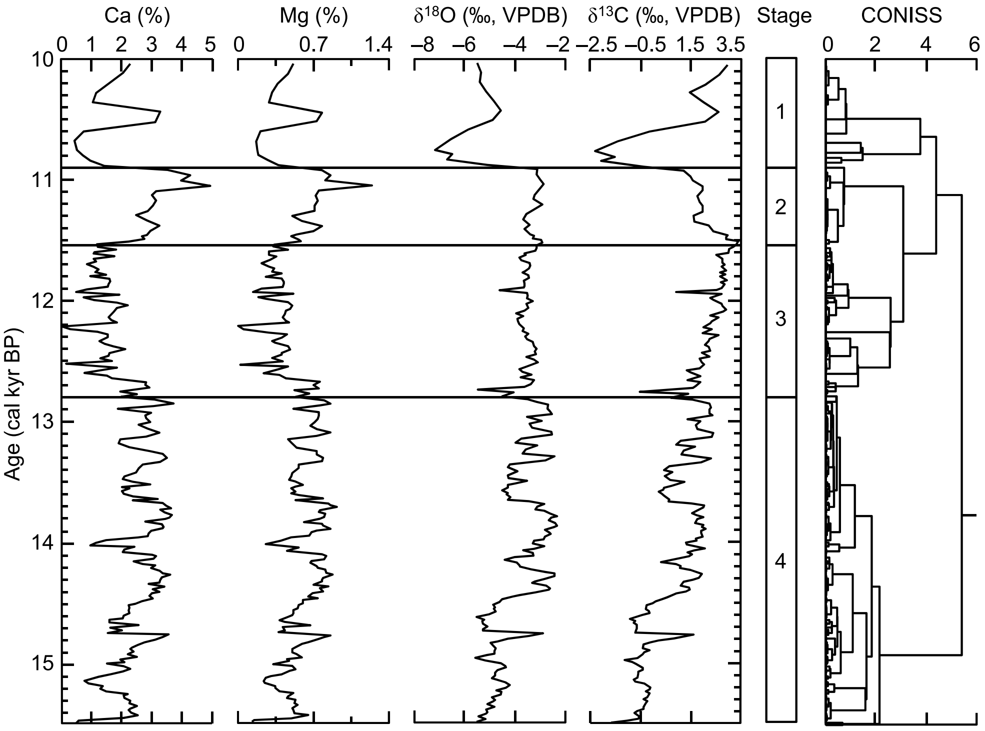

Figure 6. Time series of Ca and Mg concentrations and $\delta^{18}O$ and $\delta^{13}C$ values of <38-μm calcites from the DL04 core from 15,500 to 10,000 cal. yr BP. Ca and Mg concentrations are expressed in weight percentages in <38-μm sediments of a sample. Cluster analysis (CONISS) is based on the total sum of squares (Grimm, 1987). Horizontal solid lines indicate the major stages of changes in the data of these chemical proxies.

(Kim and O'Neil, 1997). The $\delta^{18}O$ values of endogenic calcites from the 7.71–11.83 m of the DL04 core show a large variation of up to 4.9‰ (Figure 6), implying that the water $\delta^{18}O$ values should dominate the changes in the calcite $\delta^{18}O$ values during the last deglaciation. The $\delta^{18}O$ values of the lake water are mainly controlled by the ratio of precipitation to evaporation (relative humidity) in the region and the $\delta^{18}O$ values of regional moisture related to the atmospheric temperature (+0.6‰/°C) (Dansgaard, 1964), assuming that the source water of precipitation in the region remains essentially unchanged (Liu et al., 2009; Qiang et al., 2017; Zhang et al., 2011). At present, the $\delta^{18}O$ values of the Dali Lake water are much higher than those of the inflowing rivers (Table 1), suggesting that the strong evaporation has significant influence on the enrichment in ^{18}O of the lake water (Fan et al., 2016). The intensity of evaporation in the lake region is closely related to the variations in regional temperature and precipitation. High temperature or low precipitation would be in favor of strong evaporation, which would result in high $\delta^{18}O$ values of the lake water and the endogenic calcites, and vice versa. The degree of such isotopic enrichment could be strengthened by the prolonged residence time of the lake water (Talbot, 1990). In addition, high regional temperature would produce high $\delta^{18}O$ values of regional moisture and thus of the lake water and the endogenic calcites. While significant decreases in the $\delta^{18}O$ values of endogenic calcites during the early Holocene should indicate significant increases in the isotopically lighter water input to the lake (Fan et al., 2016).

The $\delta^{13}C$ values of lacustrine endogenic calcites are mainly controlled by the $\delta^{13}C$ values of dissolved inorganic carbon (DIC) ($\delta^{13}C_{DIC}$) in the lake water which can be affected by various factors such as $\delta^{13}C$ of the inflowing riverine DIC, primary productivity of the aquatic phytoplankton, burial and degradation of the sedimentary organic matter, and isotopic exchange between the lake's DIC and atmospheric CO_2 (Leng and Marshall, 2004; Talbot, 1990). The degree of ^{13}C exchange between the lake's DIC and atmospheric CO_2 is closely related to the evaporation intensity; strong evaporation would enhance the exchange, and vice versa (Talbot, 1990). At present, the $\delta^{13}C_{DIC}$ values of the Dali Lake water are much higher than those of the inflowing rivers (Table 1), denoting that the strong evaporation contributes to the ^{13}C exchange between the lake's DIC and atmospheric CO_2, and thus the enrichment in $^{13}C_{DIC}$ of the lake water (Fan et al., 2016). The positive correlations between $\delta^{13}C$ and $\delta^{18}O$ values of endogenic calcites from the Dali Lake sediments from 15,500 to 11,550 cal. yr BP (Figure 7) indicate that the ^{13}C exchange between the lake's DIC and atmospheric CO_2 could be the dominant factor controlling variations in the $\delta^{13}C_{DIC}$ values of the lake water during that time (Talbot, 1990). Strong evaporation induced by high temperature or low precipitation would enhance the ^{13}C exchange, resulting in increases in the $\delta^{13}C_{DIC}$ values of the lake water and thus endogenic calcites in the lake sediments. In addition, prolonged water residence time of the lake would help further enrichment of $^{13}C_{DIC}$ in the lake water and thus in the endogenic calcites (Talbot, 1990). While decreases in the $\delta^{13}C$ values of endogenic calcites during the early Holocene should indicate the increases in the isotopically lighter, terrestrial carbon input to the lake (Fan et al., 2017).

Climatic change in the Dali Lake region during the last deglaciation

The high-resolution time series of the data of Ca and Mg concentrations and $\delta^{18}O$ and $\delta^{13}C$ values of endogenic calcites, together with previously published data of TOC and TN concentrations (Fan et al., 2017) from the DL04 core, can potentially be used to reconstruct the detailed history of climatic change in the Dali Lake region during the last deglaciation (Figures 6 and 8).

From 15,500 to 12,800 cal. yr BP, Ca and Mg concentrations were generally high and exhibited increasing trends, suggesting that the evaporation intensity in the region gradually increased while the dissolved CO_2 concentration in the lake water decreased related to gradual increases in regional temperature. The intervals of 15,200–15,050, 14,750–14,500, 14,100–13,900, and 13,700–13,350 cal. yr BP were marked by relatively lower regional temperature as indicated by relatively lower Ca and Mg concentrations. In addition,

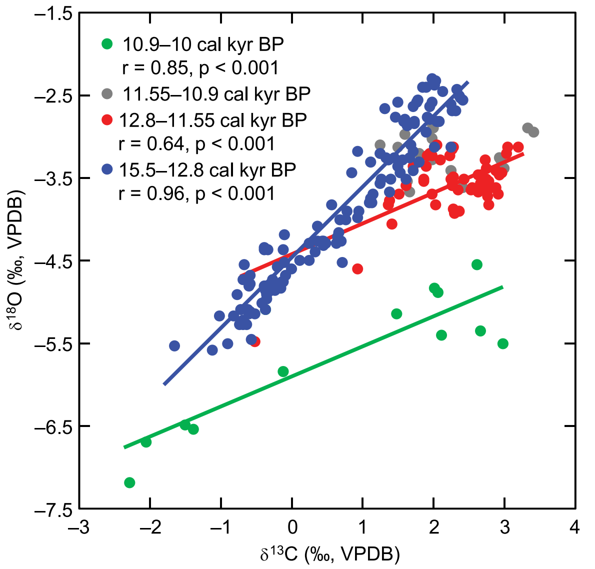

Figure 7. Relationships between $\delta^{18}O$ and $\delta^{13}C$ values of <38-μm calcites from the DL04 core from 15,500 to 10,000 cal. yr BP. The correlation coefficients (*r*) are shown for correlations statistically significant ($p \leq 0.05$).

$\delta^{18}O$ and $\delta^{13}C$ values showed similar increasing trends to Ca and Mg concentrations, supporting that regional temperature gradually increased, which resulted in the strong evaporation and high $\delta^{18}O$ values of regional moisture from 15,500 to 12,800 cal. yr BP. There were small differences in the changes between the elemental and isotopic data. For example, from 15,400 to 15,200 cal. yr BP, Ca and Mg concentrations exhibited decreasing trends, while $\delta^{18}O$ and $\delta^{13}C$ values showed increasing trends (Figure 6); from 14,100 to 14,000 cal. yr BP, the continuous decreases in Ca and Mg concentrations were in contrast to the increases in $\delta^{18}O$ and $\delta^{13}C$ values (Figure 6). These differences might be attributed to the more sensitivity of isotopes than elements in the lake water to the variations of extra factors such as decreased regional precipitation and/or humidity.

The Ca and Mg concentrations and $\delta^{18}O$ and $\delta^{13}C$ values decreased rapidly and significantly at the beginning of the period from 12,800 to 11,550 cal. yr BP, which implies that regional temperature decreased abruptly. In the rest of the period from 12,800 to 11,550 cal. yr BP, regional temperature maintained low as indicated by low Ca and Mg concentrations, while $\delta^{18}O$ and $\delta^{13}C$ values increased abruptly and then maintained high levels (Figure 6), suggesting that regional precipitation might have decreased and the water residence time of the lake might have increased. In addition, from 12,700 to 11,550 cal. yr BP, the increasing trend of $\delta^{13}C$ values was in contrast to the relatively constant $\delta^{18}O$ values (Figure 6), which may be related to the influence of low regional temperature on the low $\delta^{18}O$ values of regional moisture.

From 11,550 to 10,900 cal. yr BP, Ca and Mg concentrations increased sharply at the beginning of this period and then maintained increasing trends (Figure 6), suggesting that regional temperature increased abruptly at first and then continued to increase. $\delta^{18}O$ values increased slightly during this period, which should be related to the combined effects of increased regional temperature and increased input of ^{18}O-depleted inflowing water. The decreasing trend of $\delta^{13}C$ values from 11,550 to 10,900 cal. yr BP implies that the input of isotopically lighter, terrestrial carbon dominated the $\delta^{13}C_{DIC}$ values of the lake water and thus endogenic calcites in the lake sediments.

The Ca and Mg concentrations and $\delta^{18}O$ and $\delta^{13}C$ values decreased abruptly at the beginning of the period from 10,900 to 10,000 cal. yr BP (Figure 6), indicating that the inflowing water input to the lake increased significantly (Fan et al., 2016) and the water residence time of the lake decreased rapidly. In the rest of the period from 10,900 to 10,000 cal. yr BP, the elemental concentrations and isotopic values were generally low, with their peaks at 10,550–10,400 cal. yr BP. These data imply that the status of inflowing water input to the lake was generally high during that time, with the low interruptions at 10,550–10,400 cal. yr BP.

Previous studies on the sedimentary organic matter in Dali Lake suggested that the TOC and TN concentrations could be indicative of terrestrial inputs related to regional precipitation and biological productivity in the lake catchment related to both regional precipitation and temperature (Fan et al., 2017). Concurrent increases in the TOC and TN concentrations could indicate increases in regional precipitation and temperature (Fan et al., 2017). In general, the data of TOC and TN concentrations from the Dali Lake sediments indicated that regional precipitation and temperature gradually increased before 12,800 cal. yr BP and significantly increased after 11,550 cal. yr BP, while they slightly decreased from 12,800 to 11,550 cal. yr BP (Fan et al., 2017) (Figure 8).

Although the response of biological productivity in the Dali Lake catchment to the climatic change might be nonlinear (Fan et al., 2017), the data of Ca and Mg concentrations and $\delta^{18}O$ and $\delta^{13}C$ values of endogenic calcites, together with the data of TOC and TN concentrations from the Dali Lake sediments (Fan et al., 2017), generally delineated a warm and wet climate from 15,000 to 12,800 and from 11,550 to 10,000 cal. yr BP, and a cold and dry climate from 12,800 to 11,550 cal. yr BP (Figure 8). In addition, the temperature change was rapid and significant at the beginning and end of the period from 12,800 to 11,550 cal. yr BP (Figure 8).

Possible mechanisms for the YD event in the Dali Lake region

Previous studies on the $\delta^{18}O$ record of Greenland ice (NGRIP) (increases in the $\delta^{18}O$ values of Greenland ice indicate increases in the atmospheric temperature) indicated that there were several marked temperature fluctuations such as the Heinrich stadial 1 (H1), Bølling-Allerød (BA) warm phase, and the YD cold reversal occurring over northern high latitudes during the last deglaciation (Rasmussen et al., 2006). Among these events, the YD cold reversal (from 12,900 to 11,700 cal. yr BP) (Figure 8) is of special interest because it provides a possible similarity for the extreme events which may occur during the current global warming.

The data of elements and isotopes of endogenic calcites from the Dali Lake sediments suggested a significant cooling climate occurring in the period from 12,800 to 11,550 cal. yr BP (Figure 8). This event could be corresponded, within age uncertainties, to the YD cold reversal (Figure 8). It was suggested that the reduction in the AMOC could decrease the temperature in the NH during the YD period (Shakun and Carlson, 2010). It is likely that changes in the AMOC could have a great impact on the regional temperature in low latitude coastal areas. However, statistical data showed that the amplitude of the YD temperature anomaly increases with latitude in the NH (Shakun and Carlson, 2010), which implies that the cooling signal in northern high latitudes should have been propagated through an atmospheric teleconnection (Duan et al., 2016). In view of the abruptness of temperature change in the Dali Lake region at the beginning and end of the YD period (Figure 8), the atmosphere's dynamic propagation was proposed as the primary and direct pattern of the temperature teleconnection between the North Atlantic region and the EASM margin.

The precipitation in the Dali Lake region decreased during the YD period, which should be related to the weakening of the EASM intensity as reflected by the decreased MAP reconstructed from pollen assemblages from Gonghai Lake (38°54′ N, 112°14′ E) (Chen et al., 2015) and increased $\delta^{18}O$ values of stalagmite from Hulu Cave (32°30′ N, 119°10′ E) (Wang et al., 2001) (Figure 8).

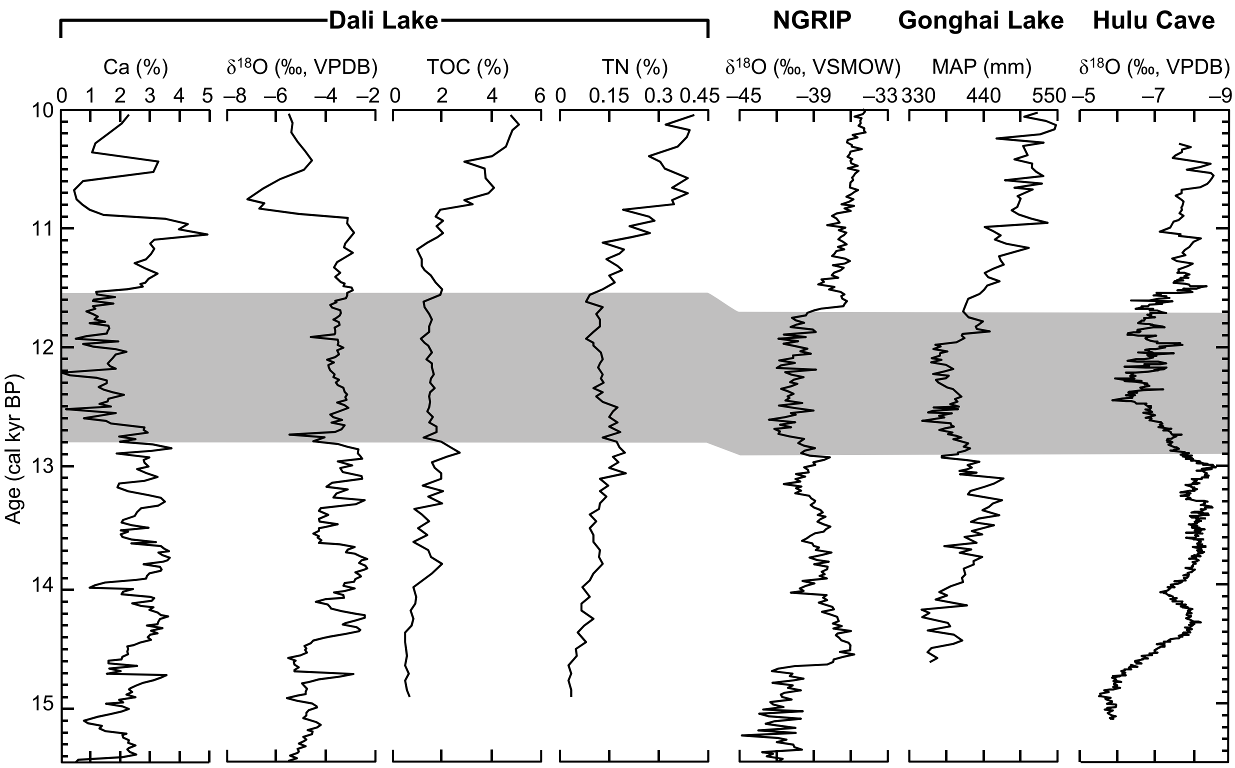

Figure 8. Correlations of Ca concentrations and $\delta^{18}O$ values of <38-μm calcites from the DL04 core from 15,500 to 10,000 cal. yr BP with TOC and TN concentrations (Fan et al., 2017) from the same sediment core, and with $\delta^{18}O$ record of Greenland ice from NGRIP (Rasmussen et al., 2006), mean annual precipitation (MAP) from Gonghai Lake (Chen et al., 2015), $\delta^{18}O$ record of stalagmite from Hulu Cave (Wang et al., 2001), respectively. Gray bar indicates the manifestation of the Younger Dryas event in the Dali Lake region.

Numerical modeling results have suggested that significant cooling in northern high latitudes could generate a low index of the North Atlantic Oscillation (NAO) and a negative index of Arctic Oscillation (AO), which would lead to a stronger flow of frigid polar air into the middle latitudes and a southward movement of the circumpolar airflow front (Bond et al., 2001; Shindell et al., 2001; Sung et al., 2006). The intensification of the circumpolar circulation over northern high latitudes could suppress the northward penetration of the EASM circulation (Sung et al., 2006), resulting in significant weakening of the monsoonal precipitation. Therefore, the decreased precipitation in the Dali Lake region should be dominantly driven by the significant cooling in northern high latitudes (Figure 8).

Dali Lake is located in the modern northern margin of the EASM (Figure 1). The tight linkage of abrupt climatic changes between the EASM margin and the northern high latitudes during the YD period may have, to some extent, been ascribed to the special geographical location of the semi-arid areas in middle latitudes for the EASM margin (Figure 1), that is far away from the monsoonal source areas but highly sensitive to the atmospheric disturbances from the northern high latitudes.

Conclusion

This study presents new high-resolution (~25 years) records of elements and stable isotopes of <38-μm calcites (endogenic calcites) from a sediment core from Dali Lake during the interval from 15.5 to 10 cal. kyr BP. The increases in Ca and Mg concentrations of the endogenic calcites are interpreted as increased evaporation intensity and decreased dissolved CO_2 concentration of the lake water, which were related to increases in regional temperature during the last deglaciation. The positive correlations between $\delta^{13}C$ and $\delta^{18}O$ values of the endogenic calcites are interpreted as the result of changes in the intensity of evaporation in the region, which were associated with the variations in regional temperature and precipitation; high temperature or low precipitation would increase the evaporation intensity and thus the $\delta^{13}C$ and $\delta^{18}O$ values of the endogenic calcites. These data indicate that the climate in the Dali Lake region was relatively warm and wet before 12,800 and after 11,550 cal. yr BP. In addition, regional temperature decreased (increased) significantly at the beginning (end) of the period from 12,800 to 11,550 cal. yr BP, and regional precipitation decreased during this period. The climatic change inferred from the elements and isotopes of the endogenic calcites from the Dali Lake sediments was generally supported by the evidence from the data of sedimentary organic matter from the same sediment core.

The abruptness of the temperature change in the Dali Lake region in the EASM margin from 12,800 to 11,550 cal. yr BP could be corresponded, within age uncertainties, to the YD cold reversal occurring over northern high latitudes. The atmospheric coupling between the North Atlantic region and the EASM margin was proposed as the dominant pattern influencing the climatic change in the Dali Lake region during the YD event.

Acknowledgements

The authors would like to thank the editor Bryan Shuman and the anonymous reviewer for the improvement of this manuscript. Jiawei Fan is grateful to Professor Mingrui Qiang for constructive suggestions on the original version of this manuscript.

Funding

This study is supported by the National Key Research and Development Program of China (2017YFA0603400), National Natural Science Foundation of China (41702179, 41130101, and 41672166), and China Postdoctoral Science Foundation (2017M610111).

References

Alley RB (2000) The Younger Dryas cold interval as viewed from central Greenland. *Quaternary Science Reviews* 19: 213–226.

An ZS (2000) The history and variability of the East Asian paleomonsoon climate. *Quaternary Science Reviews* 19: 171–187.

An ZS, Colman SM, Zhou WJ et al. (2012) Interplay between the Westerlies and Asian monsoon recorded in Lake Qinghai sediments since 32 ka. *Scientific Reports* 2: 619.

Bond G, Kromer B, Beer J et al. (2001) Persistent solar influence in North Atlantic climate during the Holocene. *Science* 294: 2130–2136.

Bond G, Showers W, Cheseby M et al. (1997) A pervasive millennial-scale cycle in North Atlantic Holocene and Glacial climates. *Science* 278: 1257–1266.

Broecker WS, Kennett JP, Flower BP et al. (1989) Routing of meltwater from the Laurentide ice sheet during the Younger Dryas cold episode. *Nature* 341: 318–321.

Chen FH, Wu D, Chen JH et al. (2016) Holocene moisture and East Asian summer monsoon evolution in the northeastern Tibetan Plateau recorded by Lake Qinghai and its environs: A review of conflicting proxies. *Quaternary Science Reviews* 154: 111–129.

Chen FH, Xu QH, Chen JH et al. (2015) East Asian summer monsoon precipitation variability since the last deglaciation. *Scientific Reports* 5: 11186.

Dansgaard W (1964) Stable isotopes in precipitation. *Tellus* 16(4): 436–468.

Dansgaard W, Johnsen SJ, Clausen HB et al. (1993) Evidence for general instability of past climate from a 250-kyr ice core record. *Nature* 364: 218–220.

Duan WH, Cheng H, Tan M et al. (2016) Onset and duration of transitions into Greenland Interstadials 15.2 and 14 in northern China constrained by an annually laminated stalagmite. *Scientific Reports* 6: 20844.

Fan JW, Xiao JL, Wen RL et al. (2016) Droughts in the East Asian summer monsoon margin during the last 6 kyrs: Link to the North Atlantic cooling events. *Quaternary Science Reviews* 151: 88–99.

Fan JW, Xiao JL, Wen RL et al. (2017) Organic geochemical investigations of the Dali Lake sediments in northern China: Implications for environment and climate changes of the last deglaciation in the East Asian summer monsoon margin. *Journal of Asian Earth Sciences* 140: 135–146.

Grimm EC (1987) CONISS: A FORTRAN 77 program for stratigraphically constrained cluster analysis by the method of incremental sum of squares. *Computers and Geosciences* 13: 13–35.

Heinrich H (1988) Origin and consequences of cyclic ice rafting in the Northeast Atlantic Ocean during the past 130,000 years. *Quaternary Research* 29: 142–152.

Hong B, Hong YT, Lin QH et al. (2010) Anti-phase oscillation of Asian monsoons during the Younger Dryas period: Evidence from peat cellulose δ13C of Hani, Northeast China. *Palaeogeography, Palaeoclimatology, Palaeoecology* 297: 214–222.

Huang XY, Meyers PA, Yu JX et al. (2012) Moisture conditions during the Younger Dryas and the early Holocene in the middle reaches of the Yangtze River, central China. *The Holocene* 22: 1473–1479.

Jiménez-López C, Romanek CS, Huertas FJ et al. (2004) Oxygen isotope fractionation in synthetic magnesian calcite. *Geochimica et Cosmochimica Acta* 68: 3367–3377.

Jin ZD, You CF, Wang Y et al. (2010) Hydrological and solute budgets of lake Qinghai, the largest lake on the Tibetan Plateau. *Quaternary International* 218: 151–156.

Johnsen SJ, Dahl-Jensen D, Gundestrup N et al. (2001) Oxygen isotope and palaeotemperature records from six Greenland ice-core stations: Camp Century, Dye-3, GRIP, GISP2, Renland and North GRIP. *Journal of Quaternary Science* 16: 299–307.

Kim ST and O'Neil JR (1997) Equilibrium and nonequilibrium oxygen isotope effects in synthetic carbonates. *Geochimica et Cosmochimica Acta* 61: 3461–3475.

Leng MJ and Marshall JD (2004) Palaeoclimate interpretation of stable isotope data from lake sediment archives. *Quaternary Science Reviews* 23: 811–831.

Lerman A (1978) *Lakes: Chemistry, Geology, Physics*. New York: Springer.

Li ZG (1993) *Annals of Hexigten Banner*. Hohhot: People's Press of Inner Mongolia (in Chinese).

Liu DB, Wang YJ, Cheng H et al. (2008) A detailed comparison of Asian monsoon intensity and Greenland temperature during the Allerød and Younger Dryas events. *Earth and Planetary Science Letters* 272: 691–697.

Liu WG, Li XZ, Zhang L et al. (2009) Evaluation of oxygen isotopes in carbonate as an indicator of lake evolution in arid areas: The modern Qinghai Lake, Qinghai-Tibet Plateau. *Chemical Geology* 268: 126–136.

Liu XJ, Colman SM, Brown ET et al. (2014) Abrupt deglaciation on the northeastern Tibetan Plateau: Evidence from Lake Qinghai. *Journal of Paleolimnology* 51: 223–240.

McManus JF, Francois R, Gherardi JM et al. (2004) Collapse and rapid resumption of Atlantic meridional circulation linked to deglacial climate changes. *Nature* 428: 834–837.

Mikolajewicz U, Crowley TJ, Schiller A et al. (1997) Modelling teleconnections between the North Atlantic and North Pacific during the Younger Dryas. *Nature* 387: 384–387.

Qiang MR, Song L, Chen FH et al. (2013) A 16-ka lake-level record inferred from macrofossils in a sediment core from Genggahai Lake, northeastern Qinghai-Tibetan Plateau (China). *Journal of Paleolimnology* 49: 575–590.

Qiang MR, Song L, Jin YX et al. (2017) A 16-ka oxygen-isotope record from Genggahai Lake on the northeastern Qinghai-Tibetan Plateau: Hydroclimatic evolution and changes in atmospheric circulation. *Quaternary Science Reviews* 162: 72–87.

Rasmussen SO, Andersen KK, Svensson AM et al. (2006) A new Greenland ice core chronology for the last glacial termination. *Journal of Geophysical Research* 111: D06102.

Russell JM, Vogel H, Konecky BL et al. (2014) Glacial forcing of central Indonesian hydroclimate since 60,000 y B.P. *Proceedings of the National Academy of Sciences of the United States of America* 111: 5100–5105.

Severinghaus JP, Sowers T, Brook EJ et al. (1998) Timing of abrupt climate change at the end of the Younger Dryas interval from thermally fractionated gases in polar ice. *Nature* 391: 141–146.

Shakun JD and Carlson AE (2010) A global perspective on Last Glacial Maximum to Holocene climate change. *Quaternary Science Reviews* 29: 1801–1816.

Shen J, Liu XQ, Wang SM et al. (2005) Palaeoclimatic changes in the Qinghai Lake area during the last 18,000 years. *Quaternary International* 136: 131–140.

Shen J, Matsumoto R, Wang SM et al. (2002) Quantitative reconstruction of the lake water paleotemperature of Daihai Lake, Inner Mongolia, China and its significance in paleoclimate. *Science in China, Series D: Earth Sciences* 45: 792–800.

Shindell DT, Schmidt GA, Mann ME et al. (2001) Solar forcing of regional climate change during the Maunder Minimum. *Science* 294: 2149–2152.

Stebich M, Mingram J, Moschen R et al. (2011) Comments on 'Anti-phase oscillation of Asian monsoons during the Younger Dryas period: Evidence from peat cellulose δ13C of Hani, Northeast China' by Hong, Y.T. Hong, Q.H. Lin, Yasuyuki Shibata, Masao Uchida, Y.X. Zhu, X.T. Leng, Y. Wang and C.C. Cai [Palaeogeography, Palaeoclimatology, Palaeoecology 297 (2010) 214–222]. *Palaeogeography, Palaeoclimatology, Palaeoecology* 310: 464–470.

Sung MK, Kwon WT, Baek HJ et al. (2006) A possible impact of the North Atlantic Oscillation on the east Asian summer monsoon precipitation. *Geophysical Research Letters* 33: L21713.

Talbot MR (1990) A review of the palaeohydrological interpretation of carbon and oxygen isotopic ratios in primary lacustrine carbonates. *Chemical Geology* 80: 261–279.

Tarasov L and Peltier WR (2005) Arctic freshwater forcing of the Younger Dryas cold reversal. *Nature* 435: 662–665.

Wang YJ, Cheng H, Edwards RL et al. (2001) A high-resolution absolute-dated late Pleistocene monsoon record from Hulu Cave, China. *Science* 294: 2345–2348.

Wunsch C (2006) Abrupt climate change: An alternative view. *Quaternary Research* 65: 191–203.

Xiao JL, Si B, Zhai DY et al. (2008) Hydrology of Dali Lake in central-eastern Inner Mongolia and Holocene East Asian monsoon variability. *Journal of Paleolimnology* 40: 519–528.

Xiao JL, Wu JT, Si B et al. (2006) Holocene climate changes in the monsoon/arid transition reflected by carbon concentration in Daihai Lake of Inner Mongolia. *The Holocene* 16: 551–560.

Xiao JL, Xu QH, Nakamura T et al. (2004) Holocene vegetation variation in the Daihai Lake region of north-central China: A direct indication of the Asian monsoon climatic history. *Quaternary Science Reviews* 23: 1669–1679.

Yancheva G, Nowaczyk NR, Mingram J et al. (2007) Influence of the intertropical convergence zone on the East Asian monsoon. *Nature* 445: 74–77.

Yang YP, Zhang HC, Chang FQ et al. (2016) Vegetation and climate history inferred from a Qinghai Crater Lake pollen record from Tengchong, southwestern China. *Palaeogeography, Palaeoclimatology, Palaeoecology* 461: 1–11.

Zhang JW, Chen FH, Holmes JA et al. (2011) Holocene monsoon climate documented by oxygen and carbon isotopes from lake sediments and peat bogs in China: A review and synthesis. *Quaternary Science Reviews* 30: 1973–1987.

Zhou X, Sun LG, Chu YX et al. (2016) Catastrophic drought in East Asian monsoon region during Heinrich event 1. *Quaternary Science Reviews* 141: 1–8.